THE JOURNAL OF BIOLOGICAL CHEMISTRY VOL. 287, NO. 10, pp. 7159–7168, March 2, 2012

An Acidic Amino Acid Transmembrane Helix 10 Residue Conserved in the Neurotransmitter:Sodium:Symporters Is Essential for the Formation of the Extracellular Gate of the γ-Aminobutyric Acid (GABA) Transporter GAT-1*

Received for publication, November 14, 2011, and in revised form, December 29, 2011 Published, JBC Papers in Press, January 10, 2012, DOI 10.1074/jbc.M111.323634

Assaf Ben-Yona and Baruch I. Kanner[1]

From the Department of Biochemistry and Molecular Biology, Institute for Medical Research Israel-Canada, Hebrew University Hadassah Medical School, Jerusalem 91120, Israel

Background: A conserved aspartate residue in the NSS family was suggested to participate in the formation of a "thin" extracellular gate.
Results: Mutation of this residue increases the proportion of outward-facing transporters.
Conclusion: This residue plays a crucial role in the gating mechanism of GAT-1.
Significance: The new insights into GAT-1 gating may be relevant for other NSS transporters.

GAT-1 mediates transport of GABA together with sodium and chloride in an electrogenic process enabling efficient GABAergic transmission. Biochemical and modeling studies based on the structure of the bacterial homologue LeuT are consistent with a mechanism whereby the binding pocket is alternately accessible to either side of the membrane and which predicts that the extracellular part of transmembrane domain 10 (TM10) exhibits aqueous accessibility in the outward-facing conformation only. In this study we have engineered cysteine residues in the extracellular half of TM10 of GAT-1 and probed their state-dependent accessibility to sulfhydryl reagents. In three out of four of the accessible cysteine mutants, the inhibition of transport by a membrane impermeant sulfhydryl reagent was diminished under conditions expected to increase the proportion of inward-facing transporters, such as the presence of GABA together with the cotransported ions. A conserved TM10 aspartate residue, whose LeuT counterpart participates in a "thin" extracellular gate, was found to be essential for transport and only the D451E mutant exhibited residual transport activity. D451E exhibited robust sodium-dependent transient currents with a voltage-dependence indicative of an increased apparent affinity for sodium. Moreover the accessibility of an endogenous cysteine to a membrane impermeant sulfhydryl reagent was enhanced by the D451E mutation, suggesting that sodium binding promotes an outward-facing conformation of the transporter. Our results support the idea that TM10 of GAT-1 lines an accessibility pathway from the extracellular space into the binding pocket and plays a role in the opening and closing of the extracellular transporter gate.

Neurotransmitter:Sodium:Symporters (NSS)[2] remove most neurotransmitters such as GABA, glycine, serotonin, dopamine, and norepinephrine from the synapses of the central nervous system and thereby play a crucial role in the communication between nerve cells (1, 2). These NSS transporters couple the flux of neurotransmitters not only to that of sodium but also to that of chloride (3–5). The first cloned NSS transporter, the GABA transporter GAT-1 (6, 7), catalyzes sodium-chloride-GABA cotransport, which is electrogenic and has a stoichiometry of 2:1:1 (3, 8–10). Although the precise order of events during a transport cycle is not yet established, it is clear that the uptake process is initiated by the binding of at least one sodium ion, which promotes capacitative transient currents in the absence of GABA (9, 11, 12). The cycle consists of different transitions, involving outward and inward facing conformations. Moreover, by analogy with the recent high resolution crystal structure of the bacterial homologue LeuT (13), conformations with the binding pocket occluded from both sides of the membrane are also likely to participate in the cycle (Fig. 1*A*).

The high resolution crystal structure of the bacterial homologue LeuT (13) appears to be an excellent model for the NSS neurotransmitter transporters (14–17). LeuT consists of 12 TMs with TMs1–5 related to TMs6–10 by a pseudo-2-fold axis in the membrane plane. The sodium ions in the binding pocket, Na1 and Na2, are both close to the substrate, which is in direct contact, through its carboxyl group, with Na1. Functional characterization of mutants of the GABA transporter GAT-1 suggest that also in this transporter the amino acid substrate participates in the Na1 site and that this site has a higher selectivity and apparent affinity for sodium than the Na2 site (14). Recently, the putative chloride binding site of the NSS neurotransmitter transporters was identified near the Na1 site (4, 5), and it was inferred that the role of chloride is mainly to

* This work was supported, in whole or in part, by grants from the Israel Science Foundation, the European Union Consortium European Drug Initiative on Channels and Transporters, and the Rosetrees Trust.
[1] To whom correspondence should be addressed: Department of Biochemistry and Molecular Biology, Hebrew University Hadassah Medical School, P. O. Box 12272, Jerusalem 91120, Israel. Tel.: 972-2-6758506; Fax: 972-2-6757379; E-mail: kannerb@cc.huji.ac.il.

[2] The abbreviations used are: NSS, Neurotransmitter:Sodium:Symporters; MTSET, (2-trimethylammonium)methanethiosulfonate; TM, transmembrane domain; GABA, γ-aminobutyric acid.

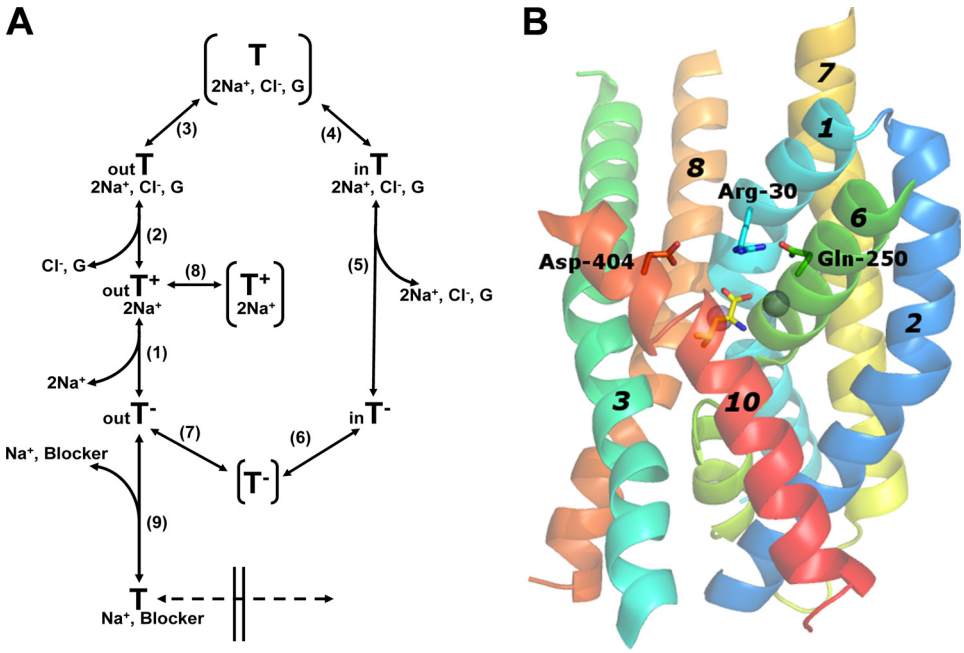

FIGURE 1. **Translocation cycle of GAT-1 and LeuT structure.** *A*, the outward facing empty transporter (out T^-) binds sodium ions (*step 1*), followed by GABA (*G*) and chloride (*step 2*) to yield the loaded outward facing transporter. This is followed by occlusion of GABA and the cotransported ions (*step 3*), and subsequently the loaded transporter becomes inward facing (*step 4*). After release of GABA and the cotransported ions to the cytoplasm (*step 5*), the empty inward facing transporter (in T^-) transits via the empty transporter, with its binding pocket occluded, to yield again the outward facing empty transporter (*steps 6* and *7*), and a new translocation cycle can begin. One of the possible scenarios for the observed transient currents could be that the outward-facing sodium-bound transporter ($outT^+_{2Na}$) becomes occluded (*step 8*). As described under "Discussion," the alternative scenario consists of *steps 6* and *7*, followed by the stabilization of ($outT^-$) by sodium (step 1). The outward facing transporter can also bind sodium ions and the blocker (*step 9*), which "locks" it in the outward conformation and prevents additional conformational changes. The sodium concentration dependence of the capacitative transient currents has been reported to be cooperative (11) and therefore we assume that both sodium ions bind to the empty outward facing transporter before GABA and chloride. The order of binding and debinding (*steps 2* and *5*) is not indicated. *B*, LeuT structure (Protein Data Bank 2A65) showing three residues involved in the formation of the "thin" extracellular gate. Bundle helices TMs 1, 2, 6, 7, as well as TMs 3, 8, and 10 are shown as indicated. Arg-30 (TM1), Gln-250 (TM6), and Asp-404 (TM10) correspond to Arg-69, Gln-291, and Asp-451 of GAT-1, respectively. The bound leucine substrate (*yellow*) and the 2 sodium ions (*spheres*) are also shown. The figure was prepared using PyMOL software.

compensate for the multiple positive charges during the substrate translocation step (5).

The conformation of LeuT is predominantly outward (extracellular)-facing with its binding pocket occluded from the cytoplasm by ~20 Å of ordered protein (13). The structure of LeuT has provided the basis for insights into the conformational changes associated with substrate translocation by a multitude of transport proteins with the same fold. Biochemical and modeling studies led to a "rocking bundle" mechanism as a framework for alternating access by NSS transporters (18). Subsequent inward-facing structures of other transporters with a similar structural fold (19, 20) are consistent with such a mechanism, which predicts that the extracellular half of TM10 is accessible to the extracellular medium in the outward-facing conformation only (18). In addition, work on the sodium-hydantoin transporter Mhp (20, 21) also indicates an important role of TM10 in its transport mechanism.

In addition to the "thick" cytoplasmic gate, the LeuT structure contains a "thin" extracellular gate where just a few highly conserved residues, a pair of conserved aromatic amino acid residues and a conserved pair composed of an aspartate residue (Asp-404) from TM10 and an arginine residue (Arg-30) from TM1 obstruct the binding pocket (13). In turn the position of the conserved arginine is stabilized by the interaction with a conserved glutamine residue (Gln-250) (13) from TM6 (Fig. 1*B*). In GAT-1 these residues are Arg-69, Gln-291, and Asp-451. Because several of the homologous residues are critical for transport in GAT-1 (22–27), it is likely that the formation of the "thin" gate is an obligate intermediate during substrate translocation: the transition from the outward- to the inward-facing conformation. Whereas conservative mutations of Arg-69 and Gln-291 were inactive in transport, both R69K and Q291N exhibited sodium-dependent transient currents (23, 27), which are thought to reflect a charge-moving conformational change associated with the binding of sodium. Interestingly, the voltage-dependence of the transient currents by both these mutants indicated an apparent increased affinity for sodium (23, 27). Unlike Arg-69 and Gln-291, the contribution of Asp-451 from GAT-1 to the function of the thin gate in GAT-1 has not yet been studied.

In this report we have addressed two related topics. We studied the possible role of Asp-451 in the gating mechanism of GAT-1, by analyzing the function of Asp-451 mutants. Moreover, using the membrane-impermeant sulfhydryl reagent MTSET, we performed a cysteine scan analysis of the external side of TM10, on which Asp-451 is located. This was done to better understand the dynamics of this domain in the context of the gating mechanism, as well as to test whether TM10 lines a conformation-dependent accessibility pathway from the extracellular side of GAT-1.

EXPERIMENTAL PROCEDURES

Generation and Subcloning of Mutants—Mutations were made by site-directed mutagenesis of GAT-1 in the vector pBluescript SK^- (Stratagene) using single-stranded uracil-containing DNA as described previously (28, 29). Briefly, the GAT-1 containing plasmid was used to transform *Escherichia coli* CJ236 (dut^-, ung^-). From one of the transformants, single-stranded uracil-containing DNA was isolated upon growth in uridine-containing medium according to the standard protocol from Stratagene, using helper phage R408. This yields the sense strand, and consequently, mutagenic primers were designed to be antisense. The mutants were subcloned into GAT-1-WT or GAT-1-C74A (a GAT-1 mutant resistant to functional impact by impermeant sulfhydryl reagents (25, 30, 31)), both residing in the vector pBluescript SK^-, using the unique restriction enzymes NheI and AgeI, and sequenced between these two restriction sites.

Cell Growth and Expression—HeLa cells were cultured in Dulbecco's-modified Eagle's medium supplemented with 10% fetal bovine serum, 200 units/ml penicillin, 200 μg/ml streptomycin, and 2 mM glutamine. Infection with recombinant vaccinia/T7 virus vTF7–3 (32) and subsequent transfection with plasmid DNA, as well as GABA transport, were done as published previously (33). The expression vector was pBluescript SK^-. Transport was performed usually for 10 min. unless indicated otherwise in the figure legends. The values for the mutants were normalized to those of GAT-1-WT or GAT-1-C74A, as indicated in the figure legends. In the experiments determining the dependence of transport on the external sodium concentration, the indicated sodium concentrations were achieved by equimolar replacement of NaCl in the transport solution (150 mM NaCl, 0.5 mM $MgSO_4$, and 5 mM KP_i, pH 7.4) with choline chloride. In all of the experiments with HeLa cells, the expression vector was pBluescript SK^-.

Inhibition Studies with Sulfhydryl Reagents—Prior to the transport assay, cells adhering to 24-well plates were washed twice with 1 ml of the transport medium containing 150 mM choline chloride instead of NaCl. Each well was then incubated at room temperature with 200 μl of the preincubation medium (the different compositions and reagent concentrations are indicated in the figure legends) with the indicated concentrations of MTSET (Anatrace). After 5 min, the medium was aspirated, and the cells were washed twice with the same solution without sulfhydryl reagents followed by [^{3}H]GABA transport. The concentration of MTSET chosen in the different experiments was optimized according to the experimental conditions of the mutants used. For instance, in Fig. 3, different concentrations were used for different mutants because some are more sensitive than others. Statistical evaluation of the inhibition of the different mutants MTSET utilized a one-way analysis of variance with a post-hoc Dunnett's multiple comparison test, where $p < 0.05$ was taken as significant. Results were plotted using normalized data for each mutant, where the untreated activity levels are normalized to 100%.

Cell Surface Biotinylation—Labeling of wild type and mutant transporters at the cell surface, using Sulfo-NHS-SS-Biotin (Pierce), quenching the reaction, cell lysis, and isolation of the biotinylated proteins by streptavidin-agarose beads (Pierce) were done as described (27). After SDS-PAGE (10% gel) and transfer to nitrocellulose, the GAT-1 protein was detected with an affinity-purified antibody, directed against an epitope from the cytoplasmic C-terminal tail of GAT-1, at a 1:500 dilution, with horseradish peroxidase-conjugated secondary antibody at a 1:40,000 dilution, and with ECL. 1% of goat serum was present in all antibody, blocking, and washing solutions to minimize the appearance of nonspecific bands.

Expression in Oocytes and Electrophysiology—cRNA was transcribed using mMESSAGE-mMACHINE (Ambion) and injected into *Xenopus laevis* oocytes, as described (23). Oocytes were placed in the recording chamber, penetrated with two agarose-cushioned micropipettes (1%/2 M KCl, resistance varied between 0.5 and 3 MΩ), voltage clamped using GeneClamp 500 (Axon Instruments) and digitized using Digidata 1322 (Axon Instruments both controlled by the pClamp9.0 suite (Axon Instruments). Voltage jumping was performed using a conventional two-electrode voltage clamp as described previously (34). The standard buffer, termed ND96, was composed of 96 mM NaCl, 2 mM KCl, 1.8 mM $CaCl_2$, 1 mM $MgCl_2$, 5 mM Na-HEPES, pH 7.5). In substitution experiments, sodium ions were replaced with equimolar choline or lithium. Treatment of oocytes, expressing GAT-1-WT or the indicated mutants, with MTSET and DTT was done exactly as described (35). The records shown in Figs. 8–10 are typical and representative of results from at least 3 oocytes. In Fig. 11, the currents were normalized as indicated in the legend to plot results of 3 oocytes as means ± S.E. Wherever error bars are not visible, the error was smaller than the size of the symbols.

RESULTS

Cysteine-scanning Mutagenesis and Impact of MTSET—Cysteines were introduced one at a time into positions 445–459 of GAT-1. According to the LeuT structure (13), these residues correspond to the extracellular side of TM10. The substitutions were made in the background of C74A, a GAT-1 mutant resistant to functional impact by impermeant sulfhydryl reagents (25, 30, 31). In two of these mutants, D451C and G457C, no measurable [^{3}H]GABA transport could be detected upon expression in HeLa cells (Fig. 2). For the other thirteen cysteine mutants, the activity ranged from 4 to 98% of that of GAT-1-WT. Because of the excellent signal to noise ratio in our experimental system, even the mutant with the lowest activity, Y445C, could be analyzed reliably for effects of MTSET on transport activity. Significant inhibition by MTSET (1 mM) was observed for 4 of the cysteine mutants: K448C, Y452C, Y453C, and S456C (Fig. 3). When alanine/serine residues were introduced at these positions instead of cysteine, no inhibition by MTSET could be observed (Fig. 4). This argues against the idea that inhibition by MTSET was due to reaction with inaccessible endogenous cysteines, exposed by the introduced mutations. Rather, it appears that the introduced cysteines themselves reacted with MTSET.

Effects of Sodium, GABA, and SKF-89976A on Reactivity toward MTSET—The residues studied are located on the extracellular side of GAT-1. If they line a permeation pathway leading from the extracellular medium to the binding pocket of the

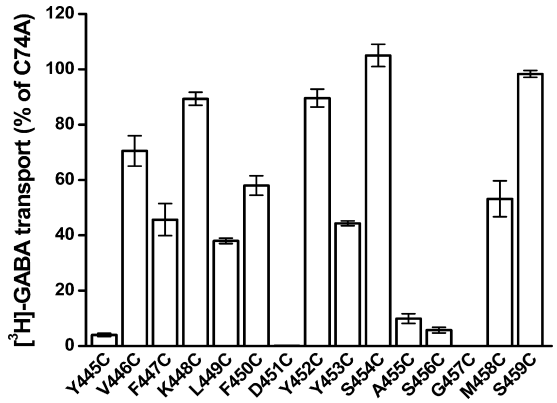

FIGURE 2. **Transport activity of cysteine mutants.** GAT-1-C74A (control) and cysteine mutants at positions 445–459 in the C74A background were transiently expressed in HeLa cells, and sodium-dependent [^{3}H]GABA transport was measured at room temperature for 10 min, as described under "Experimental Procedures." The data are given in mean ± S.E. (*error bars*) of at least three separate experiments performed in quadruplicate.

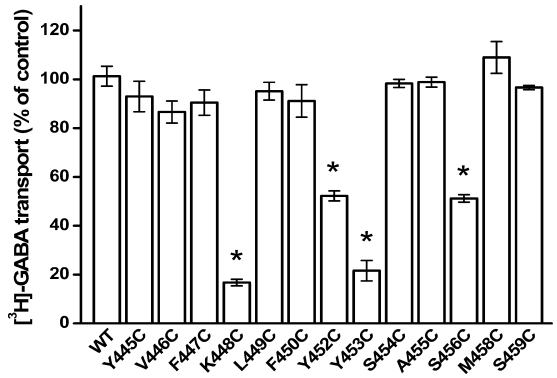

FIGURE 3. **Effect of MTSET on transport activity of cysteine mutants.** HeLa cells transiently expressing each of the indicated cysteine-mutants were pre-incubated for 5 min with transport solution containing 150 mM NaCl, with or without 1 mM MTSET, as described under "Experimental Procedures" followed by washing and [^{3}H]GABA transport. Results for each mutant are expressed as a percentage of its untreated control and represent the mean ± S.E. (*error bars*) of at least three experiments performed in quadruplicate. The means of the mutants were compared with those of C74A using a one-way analysis of variance with a post-hoc Dunnett's multiple comparison test (*, $p < 0.05$).

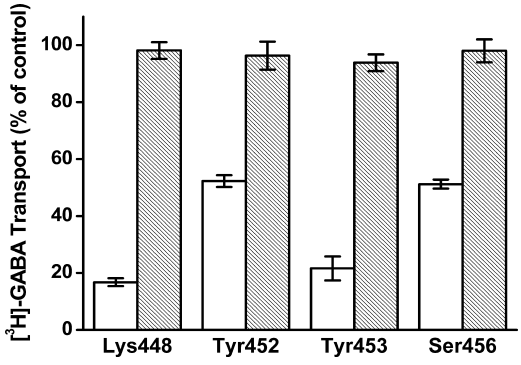

FIGURE 4. **Effect of MTSET on alanine and cysteine mutants.** The indicated cysteine (*open bars*) and alanine (*gray hatched bars*) mutants were transiently expressed in HeLa cells, and the effect of preincubation with 1 mM MTSET on transport activity was determined as described in the legend of Fig. 3. *Error bars* indicate mean ± S.E.

transporter, their accessibility is expected to increase under conditions, where the proportion of outward-facing transporters is increased. On the other hand, the opposite is expected to

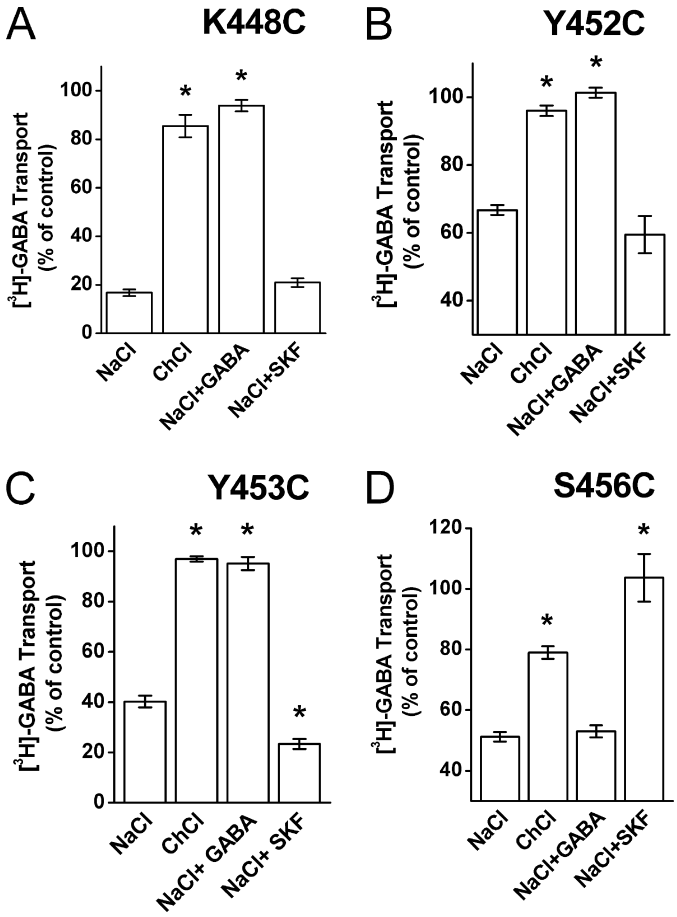

FIGURE 5. **Effect of the composition of the external medium on the inhibition of C74A/K448C, C74A/Y452C, C74A/Y453C, and C74A/S456C by MTSET.** The four indicated cysteine mutants were transiently expressed in HeLa cells. Cells were preincubated 5 min with or without MTSET in a 150 mM sodium chloride (NaCl)- or choline chloride (ChCl)-containing solution. SKF-89976A (30 μM) (SKF) and GABA (1 mM) were added as indicated. After washing, [^{3}H]GABA uptake activity was measured. Results represent the mean ± S.E. (*error bars*) of at least three experiments performed at least in quadruplicates and are given as a percentage of the uptake activity in samples preincubated in the same medium but without MTSET. For every mutant, the means of ChCl, NaCl + GABA, and NaCl + SKF were compared with those of NaCl alone, using a one-way analysis of variance with a post-hoc Dunnett's multiple comparison test (*, $p < 0.05$). The concentrations of MTSET used were 1, 0.04, 0.03, and 1 mM for K448C, Y452C, Y453C, and S456C, respectively.

be true upon increasing the proportion of inward-facing conformations. Application of GABA, in the presence of external sodium and chloride, will cause substrate translocation (Fig. 1*A*) and therefore is expected to increase the proportion of the inward-facing transporters. Indeed, when 1 mM of GABA was added during pre-incubation, a significant protection against inhibition by MTSET could be observed for three of the four MTSET-sensitive mutants, namely K448C, Y452C, and Y453C (Fig. 5, *A*, *B*, and *C*, respectively). The mere replacement of sodium by choline also resulted in a significant protection, which was observed in all 4 mutants (Fig. 5). The non-transportable GABA analog, SKF-89976A, is expected to "lock" the transporter in an outward facing conformation (Fig. 1*A*). This analog did not potentiate the inhibition of K448C and Y452C by MTSET and only slightly stimulated the inhibition of Y453C (Fig. 5, *A*–*C*), suggesting that the majority of these mutant transporters are already outward-facing in the presence of

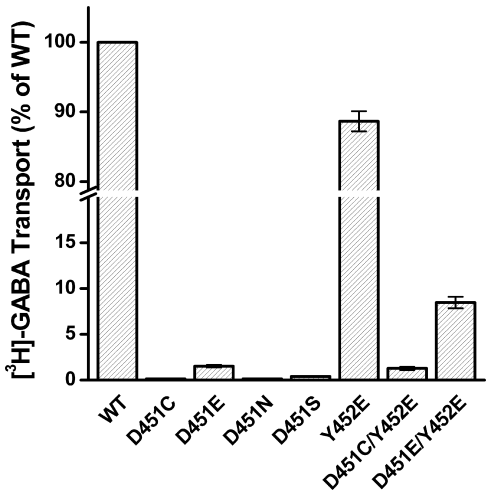

FIGURE 6. **Transport activity of Asp-451 and Tyr-452 mutants.** GAT-1-WT (control), Asp-451, and Tyr-452 mutants as well as the indicated single mutants were transiently expressed in HeLa cells, and sodium-dependent [^{3}H]GABA transport was measured at room temperature for 10 min, as described under "Experimental Procedures." The data are given in mean ± S.E. (*error bars*) of at least three separate experiments performed in quadruplicate.

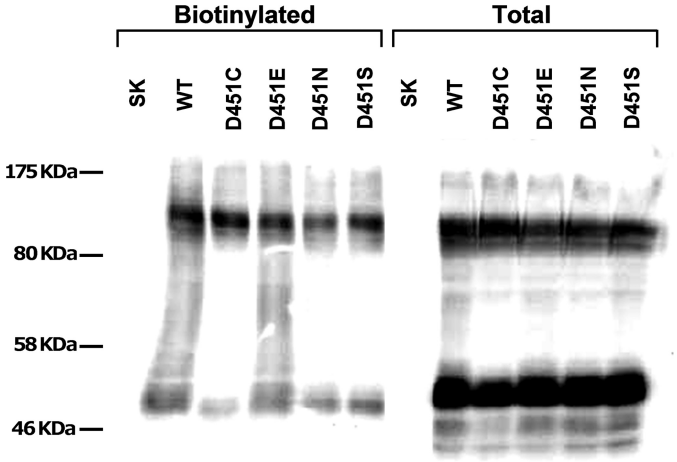

FIGURE 7. **Cell surface biotinylation of GAT-1-WT and Asp-451 mutants.** HeLa cells expressing GAT-1-WT (WT) and the indicated mutants, as well as HeLa cells transfected with the vector alone (SK), were biotinylated and processed as explained in "Experimental Procedures." The markers shown were run in the lane to the *left* of SK and contain "Prestained Protein Marker, Broad Range," Cat. # P7708S from New England Biolabs.

sodium alone. Remarkably, a significant protection by the analog, but not by GABA itself, was observed with S456C (Fig. 5*D*).

Transport by Asp-451 Mutants—When the conserved Asp-451 was replaced with cysteine, asparagine, or serine, [^{3}H]GABA transport activity was basically reduced to background levels (transfection with the vector alone, Figs. 2 and 6). Low but significant activity (1.5% ± 0.14 of WT) could be observed with the conservative replacement mutant D451E (Fig. 6), indicating the importance of the negative charge in this position. The loss of activity of the Asp-451 mutants is not due to decreased steady-state levels of the mutant transporters on the plasma membrane, because the intensity of the bands in the biotinylated fraction of these mutants is similar to WT as shown by surface-biotinylation (Fig. 7). Different from GAT-1 and from almost all known NSS members, in the serotonin transporter SERT there is a glutamate rather than an aspartate residue at position 493, which corresponds to Asp-451 of GAT-1. Moreover the adjacent residue of SERT, corresponding to Tyr-452 of GAT-1, is also a glutamate. Because it was reported that, in contrast to GAT-1-D451C, SERT-E493C retains transport activity (36), we reasoned that this may be due to the presence of the adjacent glutamate residue. Therefore we tested if the activity of the Asp-451 mutants is regained when Tyr-452 is replaced with glutamate. GAT-1 mutants Y452E, D451C/Y452E, or D451E/Y452E were generated and tested for their [^{3}H]GABA transport activity. While the Y452E mutation alone had almost no effect on transport activity (Fig. 6), a ~8.5-fold and a ~5.5-fold increase of transport could be observed when the D451C and D451E mutations were introduced into the background of Y452E, respectively (Fig. 6). Nevertheless, the activity still remained very low.

Electrophysiological Analysis of Asp-451 Mutants—As previously shown, conservative substitutions of two residues, which are predicted to participate in the formation of the "thin" extracellular gate, namely Arg-69 and Gln-291, resulted both in an impaired [^{3}H]GABA transport and the lack of GABA-induced steady-state currents (23, 27). On the other hand, both R69K and Q291N exhibited the sodium-dependent transient currents, but interestingly their voltage dependence was consistent with an increased apparent affinity for sodium (23, 27). If Asp-451 has a similar role as Arg-69 and Gln-291, one would expect to see the same "phenotype" for some of the Asp-451 substitutions. Therefore we measured transporter mediated currents of Asp-451 mutants expressed in *Xenopus laevis* oocytes. No measurable GABA-induced steady-state currents were observed with D451C, D451S, and D451N and the same was true for the sodium-dependent transient currents (data not shown). In the case of D451E, sodium-dependent transient currents were observed (Fig. 8*A*). On the other hand GABA-induced steady-state currents by D451E could not be detected (Fig. 8*B*). Nevertheless, at high concentrations, GABA could still bind to the D451E transporters because it could partly block the sodium-dependent transient currents by this mutant (Fig. 8*B*).

As in R69K and Q291N (23, 27), oocytes expressing D451E exhibited only outward transient currents in the "on" phase when jumping from a holding potential of −25 mV to more positive potentials, and no transients were observed with jumps to more negative potentials (Fig. 8*A*). These currents were capacitative, because transient currents of the same magnitude but opposite direction were seen in the "off" phase, jumping back to the holding potential (Fig. 8*A*). Like R69K and Q291N (23, 27), the voltage dependence of the transients suggest that at a holding potential of −25 mV, all of the D451E transporters are already in the sodium-bound state, indicating that these mutants have an increased apparent affinity for sodium. The bound sodium is apparently released by jumps to more positive potentials, giving rise to the outward transient currents seen in the "on" phase in Fig. 8*A*. Indeed, when the external sodium concentration was decreased, also inward transients became apparent (Fig. 8*A*). The higher apparent affinity for sodium is further illustrated by quantitative analysis of the charge movements as a function of the membrane potential. For D451E it is difficult to estimate Q_{max}, the maximal charge movement, at 100 mM sodium. This is because voltage jumps to potentials

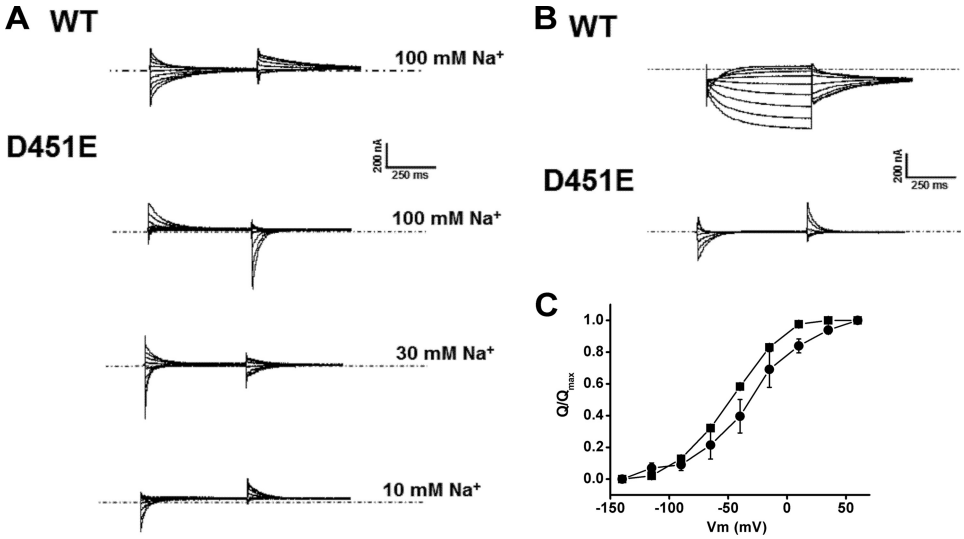

FIGURE 8. **Sodium-dependent transient currents and GABA-induced steady-state currents by GAT-WT and D451E transporters.** The membrane voltage of oocytes expressing GAT- 1-WT or D451E was stepped from a holding potential of −25 mV to voltages between −140 to +60 mV in 25-mV increments. Each potential was held clamped for 500 ms, followed by 500 ms of a potential clamped at −25 mV. All traces shown are from the same oocytes, which represent at least three repeats. *A*, transient currents, currents in 10 μM tiagabine and the indicated sodium concentration were subtracted from those in the same medium, in the absence of tiagabine. *B*, GABA-induced currents, currents in ND96 were subtracted from those in the same medium supplemented with 1 mM (GAT-1-WT) or 10 mM (D451E) of GABA. The *dashed lines* indicate zero current. Where not indicated, the external sodium concentration was 100 mM. *C*, fit of the charge movements to a Boltzmann distribution as a function of potential. The charge movements of oocytes expressing WT-GAT-1 in 100 mM sodium (■) and D451E in 30 mM sodium (●) are plotted as a function of the voltage. Charge movements were normalized to Q_{max} and were fit, using the Boltzman distribution non-linear-curve-fit function in Origin 6.1 (OriginLab Corporation). The Q_{max} values of WT and D451E were 28.2 ± 2.4 and 12.2 ± 1.0 nC, respectively. Data points are averaged from 3 oocytes for each transporter (where the S.E. is not visible, the error is smaller than the size of the symbols).

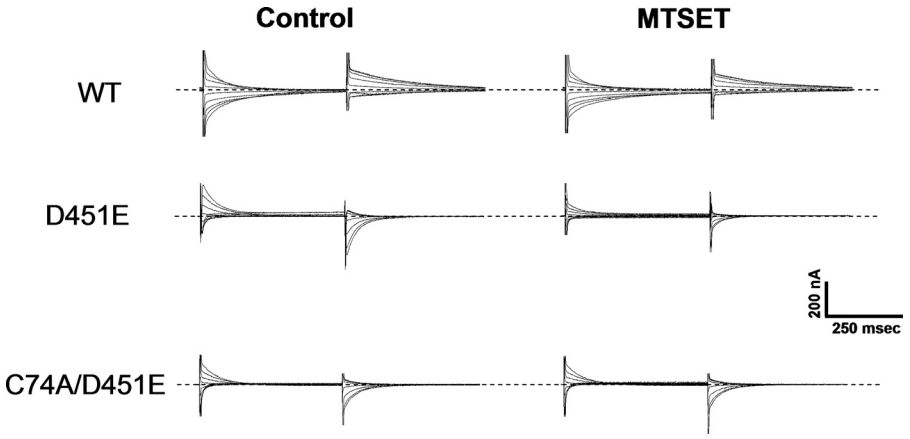

FIGURE 9. **Effect of MTSET on the transient currents of GAT-1-WT, D451E, and C74A/D451E.** Transient currents of oocytes expressing GAT-1 WT, D451E, or C74A/D451E were measured using the voltage-jump protocol described in Fig. 8. Currents in 100 mM NaCl and 10 μM tiagabine were subtracted from those recorded in the absence of tiagabine before (Control) and after a 2 min treatment with 5 mM MTSET, as described in "Experimental Procedures." Traces shown are from the same oocytes, which represent at least three repeats. The *dashed lines* indicate zero-current.

more positive than +60 mV were not tolerated well by the oocytes and at this potential the charge movement is far from complete (Fig. 8*B*). Therefore we compared the charge movements of D451E at 30 mM sodium with those of WT at 100 mM (Fig. 8*C*). The plot shows that even at 30 mM of sodium $V_{1/2}$, the voltage at which the charge movements are half completed, is more positive for D451E, −30.3 ± 1.3 mV, than for WT, −46.4 ± 1.0mV (Fig. 8*C*), even though the former was analyzed at a sodium concentration of 30 mM and the latter at 100 mM. This indicates that the apparent sodium affinity of the mutant is more than 3.3-fold higher than WT. The analysis of the charge movements also allows calculation of the value of zδ, where z is the charge on the particle moving and δ is the fraction of the membrane field through which the charge moves. Under the experimental conditions of Fig. 8*C*, the values for zδ for WT and D451E were very similar, namely 1.26 and 1.30, respectively. This is in reasonable agreement with data on WT-GAT-1 from the literature (9).

To address the question if the sodium-bound state is an occluded state, we used an indirect assay to probe the accessibility of the endogenous cysteine, Cys-74, located near the extracellular end of TM1 to the membrane impermeant positively charged sulfhydryl reagent MTSET. As noted previously, this cysteine residue is relatively unreactive (25, 30). Indeed, preincubation with the relatively high concentration of 5 mM of the sulfhydryl reagent only modestly affected the magnitude of the sodium-dependent transient currents by GAT-1-WT (Figs. 9 and 10*D*). On the other hand, under the same conditions a

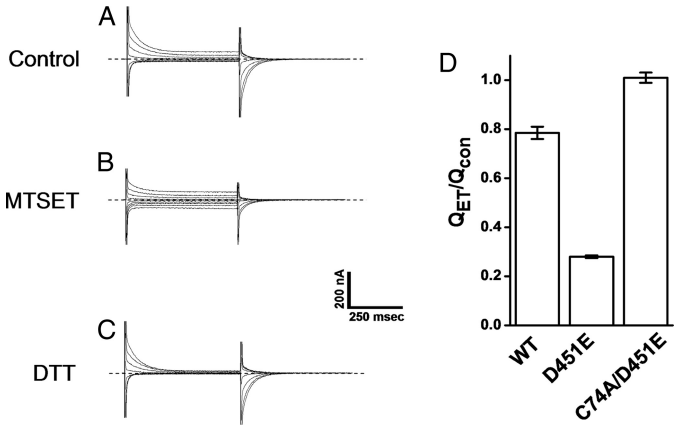

FIGURE 10. **Effects of MTSET on the transient currents of GAT-1-WT, D451E, and C74A/D451E and reversal by DTT.** *A–C*, transient currents of oocytes expressing GAT-1 D451E were measured using the voltage-jump protocol described in Fig. 8. All traces shown are from the same D451E-expressing oocyte, which represents three repeats. Currents in 100 mM NaCl and 10 μM tiagabine were subtracted from those recorded in the absence of tiagabine, before (Control) and after treatment with 5 mM MTSET and also after a subsequent exposure of the MTSET-treated oocytes to 10 mM DTT as described in "Experimental Procedures." The *dashed lines* indicate zero-current. *D*, charge movements following treatment with 5 mM MTSET were normalized to those before the exposure to the sulfhydryl reagent for GAT-1 WT, D451E, and C74A/D451E. The data are given as mean ± S.E. (*error bars*) of three oocytes.

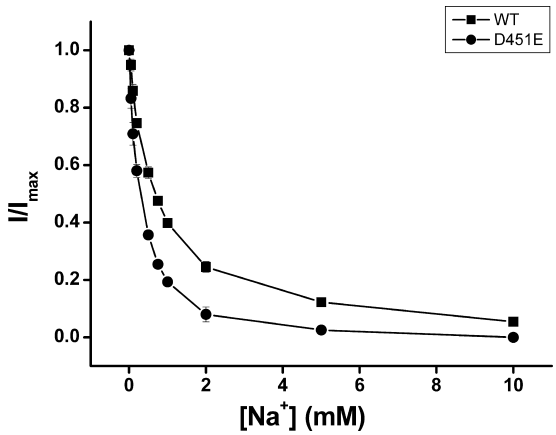

FIGURE 11. **Effects of sodium on the lithium leak currents of GAT-1-WT and D451E.** Lithium-dependent currents, obtained by subtracting the response in sodium at −140 mV, were normalized to the values for the wild type or mutant and recorded at the indicated sodium concentrations. The lithium concentration was 86.4 mM, and choline was used to maintain isoosmolarity. The data represent mean ± S.E. from three oocytes for both WT (■) and D451E (●).

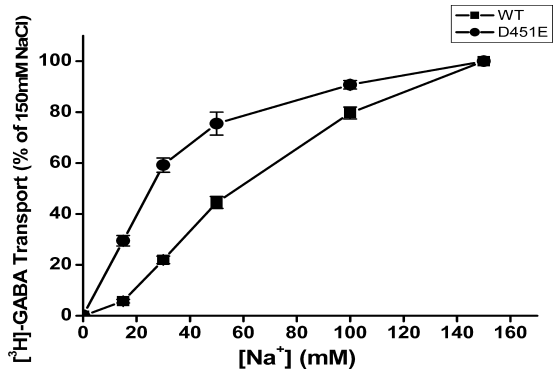

FIGURE 12. **Sodium dependence of GAT-1-WT and D451E.** HeLa cells expressing GAT-1-WT (■) and D451E (●) were assayed for [^{3}H]GABA transport as described under "Experimental Procedures." Transport was carried out for 3 min for WT and 60 min for D451E at the indicated sodium concentrations with choline as the substituting ion. The data shown at the indicated sodium concentrations are normalized to those of GAT-1-WT at 150 mM sodium (no choline substitution) or D451E, respectively and are the means ± S.E. of at least three separate experiments performed in quadruplicate.

markedly increased inhibition of the transient currents by D451E was observed (Figs. 9 and 10), consistent with the idea that at −25 mV in the presence of 100 mM Na^+, an increased proportion of the mutant transporters is outward-facing. The sodium-dependent transient currents by D451E/C74A were not sensitive to the sulfhydryl reagent (Figs. 9 and 10*D*), indicating that the inhibition of the transient currents of D451E by MTSET is indeed due to the modification of Cys-74. Treatment of the MTSET-modified mutant transporters with dithiothreitol, which is expected to restore the cysteine at position 74, also restores the sodium-dependent transient currents (Fig. 10, *A–C*).

The higher apparent affinity of D451E for sodium was also seen using a different assay. As also described for R69K (23), in parallel with the increased apparent affinity of D451E for sodium, this cation inhibited lithium leak currents of D451E (IC_{50} = 0.27 ± 0.01 mM, n = 4) at even lower concentrations than GAT-1-WT expressed in the same batches of oocytes (IC_{50} = 0.68 ± 0.02 mM, n = 3) (Fig. 11). No lithium leak currents were observed with the three other Asp-451 mutants D451C/S/N (data not shown).

Kinetic Parameters of GABA Transport by D451E—Measurement of kinetic parameters of [^{3}H]GABA transport must be performed within the linear time range of transport. For GAT-1-WT, transport is linear for the first 3 min. We reasoned that for a low activity mutant, such as D451E (Fig. 6), transport may remain linear for longer times. Time course measurements reveal that in contrast to wild-type GAT-1, where transport is no longer linear after ~6 min, the linear range for D451E is at least 75 min (data not shown). At these longer times the signal to noise ratio for the mutant was improved, so that it became feasible to determine the dependence of the initial rate of transport on the sodium concentration. We compared 60-min transport of D451E to that of 3-min transport of WT GAT-1. Also using transport as an assay, D451E exhibits a significantly higher apparent sodium affinity than WT (Fig. 12). For GAT-1-WT the $K_{0.5,Na}$ was 71.8 ± 6.0 mM and the corresponding value for D451E was 26.6 ± 1.8 mM (n = 3). When D451E was tested for its apparent substrate affinity in [^{3}H]GABA transport, the K_m for GABA was found to be of 31.7 ± 3.9 μM (n = 3), over 8-fold higher than the K_m value measured for WT −3.8 ± 0.7 μM (n = 3) Moreover, transport rate itself was dramatically impaired, as the V_{max} of D451E was only 3.2 ± 0.1% of that of WT.

DISCUSSION

The reactivity of four different cysteines, engineered at different positions of the external half of TM10 of GAT-1, to membrane impermeant MTSET (Figs. 3 and 4), indicates that this part of the domain is accessible to the aqueous extracellular space, at least in some conformations. Under conditions expected to increase the proportion of inward-facing transport-

ers, in the presence of GABA (Fig. 1*A*), the inhibition of transport by the sulfhydryl reagent was protected in three out of the four single cysteine mutants, namely K448C, Y452C, and Y453C (Fig. 5, *A–C*). A similar protection was observed in the absence of sodium, suggesting that under these conditions the transporters are predominantly inward-facing and that binding of sodium to the small proportion of "empty" outward-facing transporters (Fig. 1*A*, *step 1*) promotes more inward-facing transporters to isomerize to the outward-facing conformation (Fig. 1*A*, *steps 6* and *7* in the clockwise direction). This idea is supported by the experiments depicted in Figs. 9 and 10, which will be further discussed below. The results on the conformationally sensitive accessibility of the cysteines engineered at positions 448, 452, and 453 are compatible with the "rocking-bundle" mechanism of alternating access in the NSS transporters (18, 37). Although it remains to be seen if the structural data obtained with the sodium-hydantion symporter Mhp1 (20) are relevant for the NSS transporters, in Mhp 1 the substrate also causes a bending of TM10, prior to the large conformational change rendering the transporter inward-facing (21). Such a bending of TM10 would also be expected to reduce the aqueous accessibility of the external half of this TM. Importantly, in LeuT, molecular dynamics simulations (38) and electron paramagnetic resonance analysis in conjunction with site-directed spin labeling (39) also indicate conformational changes of TM10 during transport. The accessibility pattern of the single cysteines introduced in TM10 is not expected from a stable α-helix with only one of its side facing an aqueous access pathway. Thus, it is possible that some unwinding of this TM occurs in one of the outward-facing conformations of the transporter. Alternatively, it is possible that the cysteines engineered at positions 452 and 453 may be reached from an aqueous pocket between the external ends of TMs 10–12. In this case, one would have to assume that the spatial arrangement of this aqueous pocket changes during the transport cycle and that the modification of these cysteines interferes with these changes, resulting in an inhibition of transport (Fig. 3).

The effect of transporter ligands on the sulfhydryl modification of S456C was different from that of the three other cysteine mutants (Fig. 5*D*). In the presence of the non-transportable GABA analog, SKF-89976A, which is expected to "lock" the transporter in an outward facing conformation (Fig. 1*A*), the activity of K448C and Y452C was inhibited to the same extent by MTSET as in the presence of Na^+ alone (Fig. 5, *A* and *B*) and in the case of Y453C, the blocker slightly potentiated the inhibition (Fig. 5*C*). This again supports the idea that in the presence of Na^+, almost all of the K448C and Y452C transporters are already in the outward-facing conformation, whereas in the case of Y453C this is also true but to a lesser extent and the blocker further increases the proportion of outward-facing transporters. In the case of S456C, the bulky blocker does not potentiate but dramatically protects the modification of the engineered cysteine. This suggests that part of the ring system of the blocker is close to the side chain of Cys-456 and in fact a recent modeling study of GAT-1 indicates that part of the ring system of tiagabine, also bulky substrate analog, is located adjacent to Ser-456 (40). Unlike the other cysteine mutants (Fig. 5, *A–C*), GABA did not protect S456C from sulfhydryl modification (Fig. 5*D*). This apparent inability by GABA to increase the proportion of inward-facing transporters of S456C, may be due to intrinsic effects of the mutation on the time constants of partial reactions of the transport cycle such as a slowing of the inward translocation rate of the GABA-bound transporter (Fig. 1*A*, *steps 3* and *4*) or an increased rate of the translocation rate of the empty transporter from the intracellular to the extracellular side (Fig. 1*A*, *steps 6* and *7*).

A cysteine scan of roughly the same residues shown here was performed in the serotonin transporter SERT (36). These studies were carried out before the publication of the first LeuT structure (13) and according to the predicted topological models available at the time, the region studied was thought to represent extracellular loop 5, rather than the extracellular half of TM10. Many MTSET and MTSES accessible cysteine mutants were found, but this accessibility did not seem to be sensitive to the conformation of SERT (36), as opposed to our results with GAT-1. While we cannot exclude intrinsic mechanistic differences between GAT-1 and SERT, it is possible that the TM10 positions are also conformationally sensitive, but that the sensitivity is more difficult to detect in the SERT background. Consistent with our observations, in a recent study on the dynamics of LeuT, two TM10 positions were found where sodium increased the accessibility whereas leucine decreased it (39).

The SERT counterpart of GAT-1-D451C, E493C, retained very significant transport activity (36). Interestingly SERT, but not GAT-1, has an adjacent glutamate residue, Glu-494. Possibly, a negative charge at this position could compensate for the impact of removing the negative charge at position 493. Indeed the GABA transport activity of the D451C and D451E mutants was stimulated when Tyr-452 is replaced with glutamate (Fig. 6), but the transport activity remained nevertheless rather low. Thus this difference between SERT and GAT-1 is likely due to differences in amino acid residues at other positions.

The phenotype of the D451E mutant, namely an increased apparent affinity for Na^+ (Figs. 8, 10, and 11), is reminiscent of that of R69K (23) and of Q291N (27). This suggests that like in LeuT (13) also in GAT-1 the corresponding residues Asp-451, together with Arg-69 and Gln-291, participate in the formation of the thin extracellular gate. It has been proposed that the Na^+-dependent transient currents may reflect either the occlusion of the sodium into the interior of the transporter (2, 41) (Fig. 1*A*, *step 8*) or the reorientation of the unloaded negatively charged transporter from the inward-facing to the outward-facing conformation, followed by the stabilization of the latter by extracellular Na^+ (42) (Fig. 1*A*, *steps 6*, *7*, and *1*). The latter possibility is supported by the increased accessibility of the endogenous Cys-74 by the D451E mutation (Figs. 9 and 10*D*), which indicates that the Na^+ bound conformation is most likely outward-facing. This conclusion is also consistent with the increased accessibility of many cysteines engineered in the extracellular parts of GAT-1 TMs in the presence of Na^+ (Ref. 25) and Fig. 5, *A–C*). It is not yet clear which of the negatively charged residue(s), located in the membrane-embedded part of the transporter, could potentially move in the membrane electric field to give rise to the observed transient currents. Why is the apparent affinity of D451E for sodium higher than that of GAT-1-WT? The apparent affinity of the empty transporters

for external sodium is a function of the fraction of outward-facing transporters and the intrinsic affinity for sodium. The proportion of outward-facing D451E transporters is increased relative to GAT-1-WT (Figs. 9 and 10) and this is apparently the reason for the increased apparent affinity of the mutant transporters for sodium (Figs. 8, 11, and 12).

We postulate that the precise interplay of the residues forming the "thin" extracellular gate is critical for the large conformational changes during alternating access of both the substrate-loaded and empty transporters (Fig. 1*A*, *steps 3 + 4* and *6 + 7*, respectively). It appears likely that in D451E, where the critical negative charge at position 451 is maintained, the two translocation steps still can take place to some extent. This is probably also the reason that of the various Asp-451 mutants, only in D451E is capable of mediating sodium-dependent transient currents (Figs. 8–10) and (very slow) transport (Fig. 6). When the negative charge is eliminated by mutation, the function of the "thin" extracellular gate is presumably affected so much that inward-outward transitions of the unloaded and fully unloaded transporters cannot take place anymore. The fact that the other Asp-451 mutants are not even able to mediate the lithium leak currents, suggests that the appropriate interaction of the residues of the "thin" external gate is also required for this process.

Acknowledgments—We thank Elia N. Zomot for the initial characterization of the Asp-451 mutants and Niels C. Danbolt for the affinity-purified antibody against GAT-1.

REFERENCES

1. Nelson, N. (1998) The family of Na^+/Cl^- neurotransmitter transporters. *J. Neurochem.* **71,** 1785–1803
2. Kanner, B. I., and Zomot, E. (2008) Sodium-coupled neurotransmitter transporters. *Chem. Rev.* **108,** 1654–1668
3. Keynan, S., and Kanner, B. I. (1988) γ-Aminobutyric acid transport in reconstituted preparations from rat brain: coupled sodium and chloride fluxes. *Biochemistry* **27,** 12–17
4. Forrest, L. R., Tavoulari, S., Zhang, Y. W., Rudnick, G., and Honig, B. (2007) Identification of a chloride ion binding site in Na^+/Cl^--dependent transporters. *Proc. Natl. Acad. Sci. U.S.A.* **104,** 12761–12766
5. Zomot, E., Bendahan, A., Quick, M., Zhao, Y., Javitch, J. A., and Kanner, B. I. (2007) Mechanism of chloride interaction with neurotransmitter: sodium symporters. *Nature* **449,** 726–730
6. Radian, R., Bendahan, A., and Kanner, B. I. (1986) Purification and identification of the functional sodium- and chloride-coupled γ-aminobutyric acid transport glycoprotein from rat brain. *J. Biol. Chem.* **261,** 15437–15441
7. Guastella, J., Nelson, N., Nelson, H., Czyzyk, L., Keynan, S., Miedel, M. C., Davidson, N., Lester, H. A., and Kanner, B. I. (1990) Cloning and expression of a rat brain GABA transporter. *Science* **249,** 1303–1306
8. Kavanaugh, M. P., Arriza, J. L., North, R. A., and Amara, S. G. (1992) Electrogenic uptake of γ-aminobutyric acid by a cloned transporter expressed in *Xenopus* oocytes. *J. Biol. Chem.* **267,** 22007–22009
9. Mager, S., Naeve, J., Quick, M., Labarca, C., Davidson, N., and Lester, H. A. (1993) Steady states, charge movements, and rates for a cloned GABA transporter expressed in *Xenopus* oocytes. *Neuron* **10,** 177–188
10. Lu, C. C., and Hilgemann, D. W. (1999) GAT1 (GABA:Na^+:Cl^-) cotransport function. Steady state studies in giant *Xenopus* oocyte membrane patches. *J. Gen Physiol.* **114,** 429–444
11. Mager, S., Kleinberger-Doron, N., Keshet, G. I., Davidson, N., Kanner, B. I., and Lester, H. A. (1996) Ion binding and permeation at the GABA transporter GAT1. *J. Neurosci.* **16,** 5405–5414
12. Hilgemann, D. W., and Lu, C. C. (1999) GAT1 (GABA:Na+:Cl-) cotransport function. Database reconstruction with an alternating access model. *J. Gen Physiol.* **114,** 459–475
13. Yamashita, A., Singh, S. K., Kawate, T., Jin, Y., and Gouaux, E. (2005) Crystal structure of a bacterial homologue of Na+/Cl– dependent neurotransmitter transporters. *Nature* **437,** 215–223
14. Zhou, Y., Zomot, E., and Kanner, B. I. (2006) Identification of a lithium interaction site in the γ-aminobutyric acid (GABA) transporter GAT-1. *J. Biol. Chem.* **281,** 22092–22099
15. Zhang, Y. W., and Rudnick, G. (2006) The cytoplasmic substrate permeation pathway of serotonin transporter. *J. Biol. Chem.* **281,** 36213–36220
16. Vandenberg, R. J., Shaddick, K., and Ju, P. (2007) Molecular basis for substrate discrimination by glycine transporters. *J. Biol. Chem.* **282,** 14447–14453
17. Dodd, J. R., and Christie, D. L. (2007) Selective amino acid substitutions convert the creatine transporter to a γ-aminobutyric acid transporter. *J. Biol. Chem.* **282,** 15528–15533
18. Forrest, L. R., Zhang, Y. W., Jacobs, M. T., Gesmonde, J., Xie, L., Honig, B. H., and Rudnick, G. (2008) Mechanism for alternating access in neurotransmitter transporters. *Proc. Natl. Acad. Sci. U.S.A.* **105,** 10338–10343
19. Faham, S., Watanabe, A., Besserer, G. M., Cascio, D., Specht, A., Hirayama, B. A., Wright, E. M., and Abramson, J. (2008) The crystal structure of a sodium galactose transporter reveals mechanistic insights into Na+/sugar symport. *Science* **321,** 810–814
20. Shimamura, T., Weyand, S., Beckstein, O., Rutherford, N. G., Hadden, J. M., Sharples, D., Sansom, M. S., Iwata, S., Henderson, P. J., and Cameron, A. D. (2010) Molecular basis of alternating access membrane transport by the sodium-hydantoin transporter Mhp1. *Science* **328,** 470–473
21. Weyand, S., Shimamura, T., Yajima, S., Suzuki, S., Mirza, O., Krusong, K., Carpenter, E. P., Rutherford, N. G., Hadden, J. M., O'Reilly, J., Ma, P., Saidijam, M., Patching, S. G., Hope, R. J., Norbertczak, H. T., Roach, P. C., Iwata, S., Henderson, P. J., and Cameron, A. D. (2008) Structure and molecular mechanism of a nucleobase-cation-symport-1 family transporter. *Science* **322,** 709–713
22. Pantanowitz, S., Bendahan, A., and Kanner, B. I. (1993) Only one of the charged amino acids located in the transmembrane α-helices of the γ-aminobutyric acid transporter (subtype A) is essential for its activity. *J. Biol. Chem.* **268,** 3222–3225
23. Kanner, B. I. (2003) Transmembrane domain I of the gamma-aminobutyric acid transporter GAT-1 plays a crucial role in the transition between cation leak and transport modes. *J. Biol. Chem.* **278,** 3705–3712
24. Bismuth, Y., Kavanaugh, M. P., and Kanner, B. I. (1997) Tyrosine 140 of the γ-aminobutyric acid transporter GAT-1 plays a critical role in neurotransmitter recognition. *J. Biol. Chem.* **272,** 16096–16102
25. Rosenberg, A., and Kanner, B. I. (2008) The substrates of the γ-aminobutyric acid transporter GAT-1 induce structural rearrangements around the interface of transmembrane domains 1 and 6. *J. Biol. Chem.* **283,** 14376–14383
26. Mari, S. A., Soragna, A., Castagna, M., Santacroce, M., Perego, C., Bossi, E., Peres, A., and Sacchi, V. F. (2006) Role of the conserved glutamine 291 in the rat γ-aminobutyric acid transporter rGAT-1. *Cell Mol Life Sci* **63,** 100–111
27. Ben-Yona, A., Bendahan, A., and Kanner, B. I. (2011) A glutamine residue conserved in the neurotransmitter:sodium:symporters is essential for the interaction of chloride with the GABA transporter GAT-1. *J. Biol. Chem.* **286,** 2826–2833
28. Kunkel, T. A., Roberts, J. D., and Zakour, R. A. (1987) Rapid and efficient site-specific mutagenesis without phenotypic selection. *Methods Enzymol.* **154,** 367–382
29. Kleinberger-Doron, N., and Kanner, B. I. (1994) Identification of tryptophan residues critical for the function and targeting of the γ-aminobutyric acid transporter (subtype A). *J. Biol. Chem.* **269,** 3063–3067
30. Bennett, E. R., and Kanner, B. I. (1997) The membrane topology of GAT-1, a (Na^+ + Cl^-)-coupled γ-aminobutyric acid transporter from rat brain. *J. Biol. Chem.* **272,** 1203–1210
31. Golovanevsky, V., and Kanner, B. I. (1999) The reactivity of the γ-aminobutyric acid transporter GAT-1 toward sulfhydryl reagents is confor-

mationally sensitive. Identification of a major target residue. *J. Biol. Chem.* **274,** 23020–23026
32. Fuerst, T. R., Niles, E. G., Studier, F. W., and Moss, B. (1986) Eukaryotic transient-expression system based on recombinant vaccinia virus that synthesizes bacteriophage T7 RNA polymerase. *Proc. Natl. Acad. Sci. U.S.A.* **83,** 8122–8126
33. Keynan, S., Suh, Y. J., Kanner, B. I., and Rudnick, G. (1992) Expression of a cloned γ-aminobutyric acid transporter in mammalian cells. *Biochemistry* **31,** 1974–1979
34. Borre, L., and Kanner, B. I. (2004) Arginine 445 controls the coupling between glutamate and cations in the neuronal transporter EAAC-1. *J. Biol. Chem.* **279,** 2513–2519
35. Borre, L., Kavanaugh, M. P., and Kanner, B. I. (2002) Dynamic equilibrium between coupled and uncoupled modes of a neuronal glutamate transporter. *J. Biol. Chem.* **277,** 13501–13507
36. Keller, P. C., 2nd, Stephan, M., Glomska, H., and Rudnick, G. (2004) Cysteine-scanning mutagenesis of the fifth external loop of serotonin transporter. *Biochemistry* **43,** 8510–8516
37. Forrest, L. R., and Rudnick, G. (2009) The rocking bundle: a mechanism for ion-coupled solute flux by symmetrical transporters. *Physiology* **24,** 377–386
38. Zhao, Y., Terry, D. S., Shi, L., Quick, M., Weinstein, H., Blanchard, S. C., and Javitch, J. A. (2011) Substrate-modulated gating dynamics in a Na^+-coupled neurotransmitter transporter homologue. *Nature* **474,** 109–113
39. Claxton, D. P., Quick, M., Shi, L., de Carvalho, F. D., Weinstein, H., Javitch, J. A., and McHaourab, H. S. (2010) Ion/substrate-dependent conformational dynamics of a bacterial homolog of neurotransmitter:sodium symporters. *Nat. Struct Mol. Biol.* **17,** 822–829
40. Skovstrup, S., Taboureau, O., Bräuner-Osborne, H., and Jørgensen, F. S. (2010) Homology modeling of the GABA transporter and analysis of tiagabine binding. *Chem. Med. Chem.* **5,** 986–1000
41. Lu, C. C., and Hilgemann, D. W. (1999) GAT1 (GABA:Na+:Cl-) cotransport function. Kinetic studies in giant *Xenopus* oocyte membrane patches. *J. Gen Physiol.* **114,** 445–457
42. Loo, D. D., Hazama, A., Supplisson, S., Turk, E., and Wright, E. M. (1993) Relaxation kinetics of the Na^+/glucose cotransporter. *Proc. Natl. Acad. Sci. U.S.A.* **90,** 5767–5771